Journal of Mining and Metallurgy, 61 A (1) (2025) 73-81

Research paper

https://doi:10.5937/JMMA2501073M

Journal of Mining and Metallurgy

STELLERITE-STILBITE AND CALCITE PARAGENESIS IN A FRACTURE CAVITY HOSTED BY ANDESITIC VOLCANICLASTIC ROCKS FROM THE TIMOK MAGMATIC COMPLEX

D. Medić[1#], Z. Štirbanović[1], M. Banješević[1], V. Nedelkovski[1], S. Stanković[1], A. Cvetković[1], S. Đorđievski[2]

[1]University of Belgrade, Technical Faculty in Bor, Bor, Serbia
[2]Mining and Metallurgy Institute Bor, Bor, Serbia

Received: October 3, 2025; Accepted: December 2, 2025

Abstract

The Timok Magmatic Complex (TMC) is part of the Apuseni–Banat–Timok–Srednogorie magmatic arc within the Tethyan metallogenic belt, hosting world-class porphyry and epithermal copper–gold deposits. In a bedrock channel of the Šarbanovac River (central part of the TMC), seasonal desiccation exposed a fracture cavity within Upper Cretaceous andesitic volcaniclastic rocks, revealing white and yellow mineral aggregates inside the cavity and green mineral aggregates in the surrounding wall rock. X-ray powder diffraction (XRPD) analyses of separated fractions show that the yellow crystals are stellerite-stilbite zeolites, while the white crystals are calcite. The surrounding green wall rock contains quartz, glauconite, clinochlore, and epistilbite. Quartz represents relict magmatic grains incorporated into the volcaniclastic deposit, while glauconite and clinochlore reflect early diagenetic to propylitic alteration. Epistilbite occurs within pores and microfractures, indicating local wall-rock zeolitization predating the main fracture mineralization. Stellerite-stilbite was first deposited along the fracture walls, followed by calcite filling the central part of the cavity, forming a characteristic layered ("sandwich") texture. These findings document a multistage paragenetic history involving early diagenetic alteration of porous volcaniclastic material, secondary zeolitization, tectonically induced fracturing, and late-stage low-temperature hydrothermal mineralization. This study provides a rare example of fracture-controlled zeolite-carbonate paragenesis preserved in situ within exposed volcaniclastic bedrock of the TMC.

Key words: *Volcaniclastite, andesite, fracture, stilbite, stellerite, calcite.*

1. Introduction

The Balkan–Carpathian region is one of Europe's most important metallogenic provinces and is part of the larger Tethyan metallogenic belt. Within this belt, porphyry and epithermal copper–gold systems are common, indicating a complex geodynamic history of subduction, collision, and post-collisional magmatism [1], [2]. These processes have created some of Europe's largest ore deposits, including major copper and gold resources in Romania, Serbia and Bulgaria. Consequently, the region has been the focus of extensive geological and metallogenic research for many years, especially regarding the connection between magmatic evolution, structural controls, and hydrothermal alteration in ore formation [1], [3].

The Timok Magmatic Complex (TMC) in Eastern Serbia represents one of the most prominent segments of this metallogenic belt. It is predominantly composed of Upper Cretaceous volcanic and subvolcanic rocks (andesites, dacites, less often basaltic andesites and rhyolites, and their volcaniclastites), as well as intrusive bodies genetically related to porphyry and epithermal mineralization [4], [5], [6]. Its economic importance is reflected in major deposits such as Bor, Majdanpek, Čukaru Peki, and Veliki Krivelj, which have been exploited for over a century and continue to attract global attention as sites of active production and exploration [2], [7], [8]. From a geodynamic perspective, the TMC records multiphase magmatic activity associated with the evolution of the Apuseni–Banat–Timok–Srednogorie (ABTS) magmatic arc, reflecting the spatial and temporal migration of magmatism and hydrothermal systems across the Balkan–Carpathian region [9], [10].

[#]***Corresponding author:*** dmedic@tfbor.bg.ac.rs

Magmatism is separated into three volcanic phases, where the first phase (dominated by andesitic rocks) is the most significant economically because it is the host rock of the largest porphyry Cu and Au deposits [2], [4], [6].

The mineral composition of the andesites from the TMC reflects the typical features of intermediate magmas and the petrogenetic conditions of this segment of the ABTS magmatic arc. Petrographic studies indicate that the essential minerals are plagioclase and hornblende, often occurring as coarse-grained phenocrysts, whereas quartz and biotite appear in subordinate amounts [4], [5], [11], [12]. Accessory minerals include magnetite, apatite, zircon, and titanium-oxide minerals, which play a key role in reconstructing crystallization conditions and in geochronological analyses, as zircons record crystallization ages between 89 and 82 Ma and confirm the genetic link between the first volcanic phase and the formation of porphyry and epithermal copper–gold deposits in Bor and Čukaru Peki [2], [4]. In addition to these primary and accessory phases, secondary minerals may occur, representing hydrothermal products.

Hydrothermal alteration represents a fundamental process in the geological evolution of the TMC, closely linked to the formation of porphyry and epithermal Cu–(Au) deposits during the Late Cretaceous [13], [14], [15]. High-temperature magmatic–hydrothermal fluids circulated through the andesitic to dacitic volcanic and subvolcanic rocks, generating extensive alteration halos and ore bodies. These fluids were characterized by elevated temperatures, high pressures, and acidic to near-neutral pH, and were rich in sulfur, iron, and copper, enabling the formation of sulfide assemblages dominated by pyrite and chalcopyrite. Alteration zones show systematic zonation, including potassic, sericitic, silicic, and propylitic domains, reflecting gradients in temperature, pH, and fluid composition [2]. In contrast, hydrothermal fluids active during the Neogene to Quaternary were cooler, neutral to slightly alkaline, and characterized by low contents of dissolved metals. Hydrothermal activity is evidenced today by thermal springs in the region, such as Šarbanovac, Sumrakovac, and Brestovac Spa, which discharge waters of 30–40 °C, reflecting ongoing shallow hydrothermal circulation.

From a geomorphological perspective, the distinction between alluvial and bedrock channels has important implications for sediment transport, channel incision, and the visibility of geological structures. Alluvial channels are typically mantled by unconsolidated sand and gravel derived from the upstream catchment [16], and their sediment composition reflects an integrated lithological signal of the entire drainage basin [17], [18]. In contrast, bedrock channels form where the transport capacity of the river exceeds the sediment supply, leaving little or no alluvial cover [19], [20], [21]. Such settings provide direct exposure of rocks in the channel floor, offering a unique opportunity to investigate local mineral associations and parageneses that are specific to the site. The Šarbanovac River represents such a bedrock channel, where seasonal desiccation allows direct access to otherwise hidden mineralization. This distinction is critical when interpreting sediment geochemistry and mineralogical variability, as it determines whether the observed material represents a regional average of upstream lithologies or localized bedrock features.

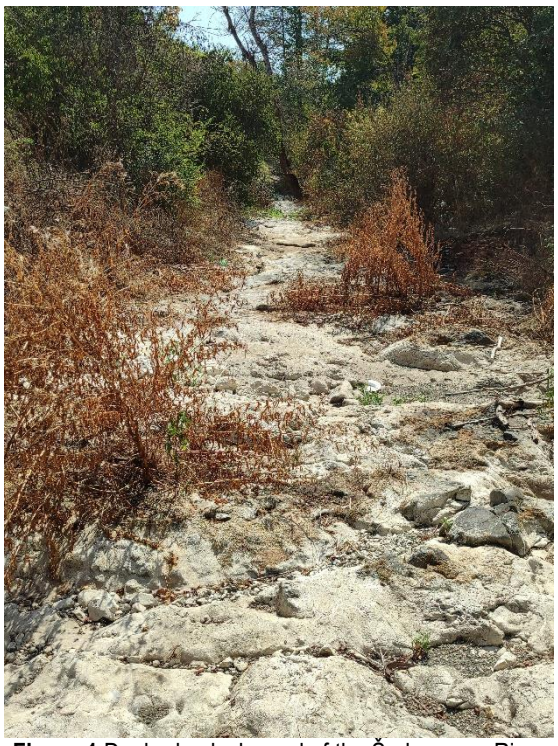

Figure 1 Dry bedrock channel of the Šarbanovac River on 18 August 2024

The Šarbanovac River, a small tributary draining the TMC, provides an illustrative example. It is about 18 km long, with a catchment area of approximately 36 km². In the upper part of the basin, the river flows over Upper Cretaceous volcaniclastic rocks of hornblende and augite–hornblende andesites composition, while in the lower basin Neogene conglomerates, sandstones, and

marls dominate. There are no mining or metallurgical facilities, nor other significant pollution sources within the catchment. In one section of the upper basin, the Šarbanovac River incises directly into bedrock. The river undergoes seasonal desiccation, leaving parts of its bed completely dry. During low-flow conditions, bedrock is exposed in the channel floor, with rock formations clearly visible (Figure 1). This makes the Šarbanovac River a rare locality where geomorphic processes reveal otherwise inaccessible characteristics of the underlying bedrock.

At certain locations within the bed of the Šarbanovac River, fractures in andesitic rocks are visible, containing white and yellow crystals, as well as green-colored rocks occurring further away from the fractures. These features represent a rare opportunity to study fracture fillings and associated mineral assemblages in their natural geomorphic setting. This study aims to identify the minerals within the fractures and their immediate surroundings using *X-ray powder diffraction (XRPD)* analysis, and to describe their textural characteristics, composition, and discuss paragenetic relationships. Based on the obtained results, the study aims not only to reconstruct the specific environmental conditions that led to their formation but also to provide new insights into the late stages of low-temperature hydrothermal alteration in the TMC.

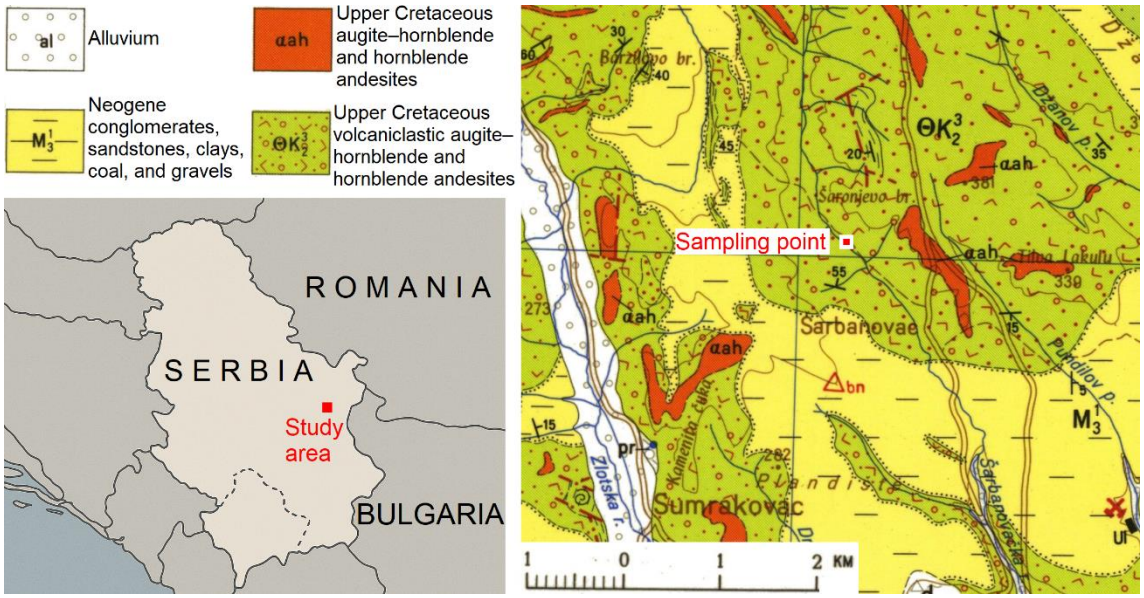

Figure 2 Location of the sampling point is shown on the part of the geological map, sheet Zaječar 1:100.000 [22]. The inset on the left shows the study area on a simplified geographic map

2. Experimental

2.1. Sampling

Samples were collected on 18 August 2024 at an exposed fracture within an andesitic bedrock outcrop in the channel of the Šarbanovac River (TMC), at coordinates N 43.969607, E 22.063967. Figure 2 shows the geological setting of the study area within the TMC and the location of the sampling site in the Šarbanovac River basin. The sampling site was fully dry at the time of collection, following seasonal desiccation of the river, which provided unobstructed access to the channel floor. Sampling was carried out manually, without specialized equipment, as the fracture-filling material (Figure 3a) could be removed by hand. A single "sandwich-like" piece was detached directly from the fracture, exposing white crystals in the center and yellow crystals on both sides (Figure 3b). A separate greenish sample was collected from the wall rock adjacent to the fracture (Figure 3e).

2.2. Sample preparation

The collected samples were transferred to the Mining and Metallurgy Institute Bor, where they were prepared for further analyses.

In the laboratory, the fracture-filling sample was crushed and manually separated into white and yellow crystalline fractions without the use of magnification, as

the crystals were sufficiently large to be distinguished and separated by the naked eye (Figure 3c and 3d). Each fraction, as well as the green wall-rock sample, was individually ground in an agate mortar to a fine powder suitable for X-ray diffraction (XRPD) analysis. The powders were then mounted on standard sample holders, with care taken to produce smooth surfaces to minimize preferred orientation effects. No drying was required, as all samples were collected in dry conditions.

2.3. XRPD analyses

XRPD analyses were performed using a Rigaku MiniFlex 600 diffractometer equipped with a D/teX Ultra 250 high-speed detector and a Cu Kα X-ray tube. Data were collected over a 2θ range of 3–90°, with a step size of 0.02° and a scanning speed of 10° min^{-1}. The generator settings were 40 kV and 15 mA. Mineral phases were identified using PDXL 2 software (Version 2.4.2.0), and diffraction patterns were matched by the ICDD PDF-2 (2015) database. The detection limit of the XRPD analysis is approximately 1 wt.%, and the results provide semi-quantitative estimates of mineral abundance in each sample.

To facilitate data organization, the three samples were assigned internal codes: Y (yellow fracture-filling crystals), W (white fracture-filling crystals), and G (green wall rock). This nomenclature is used consistently in the Results and Discussion section. The analytical strategy – separating field-identified textural zones and analyzing them individually – was chosen to reflect the field-observed zonation within the fracture cavity and to link mineralogical data with the geomorphic and structural setting.

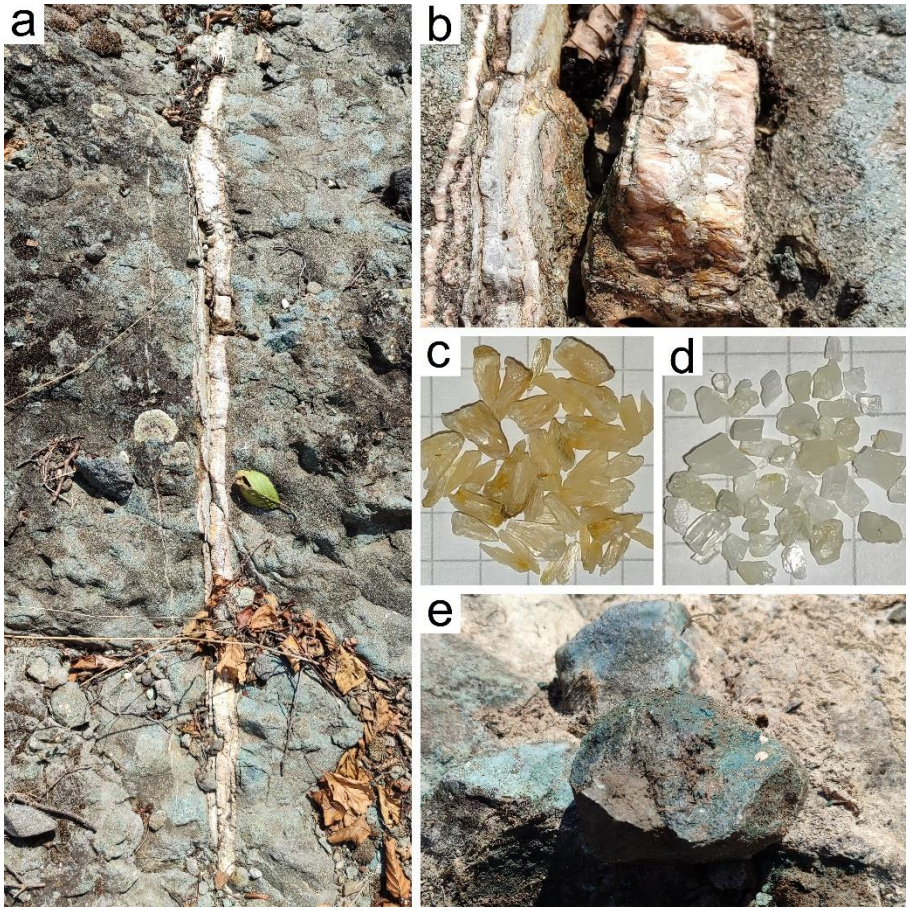

Figure 3 a) Fracture in the andesitic volcanoclastic rock from the TMC, b) Close-up image of the mineral assemblage from the fracture cavity, c) Sample Y (yellow fracture-filling crystals), d) Sample W (white fracture-filling crystals) e) Sample G (green wall rock)

3. Results and discussion

3.1. Mineralogical assemblage in the fracture cavity

The mineralogical assemblage within the fracture cavity consists predominantly of calcite and stellerite. The yellow crystals (sample Y) are composed of stellerite ($Ca_2Al_4Si_{14}O_{36}\cdot 14H_2O$), whose diffraction pattern (Figure 4) matches the reference ICDD card 00-025-0124 [23]. The strongest diffraction maxima are: d = 9.05 Å (020), d = 4.05 Å (133), and d = 3.03 Å (153).

The white crystals (sample W) consist mainly of calcite ($CaCO_3$), as indicated by the strongest diffraction maxima at d = 3.03 Å (104), d = 2.28 Å (113), and d = 2.09 Å (202) (Figure 5). These values agree well with those of the reference pattern ICDD 01-080-2802 [24].

Minor reflections attributable to stellerite are also observed in the white-crystal pattern, particularly at low angles around d = 9.08 Å (020), d = 4.05 Å (133), and d = 2.84 Å (026). This small zeolite component is interpreted not as a true mixed paragenesis, but as contamination resulting from manual separation of crystals: during hand-picking, a minor amount of yellow zeolite crystals was inadvertently included with the white calcite crystals.

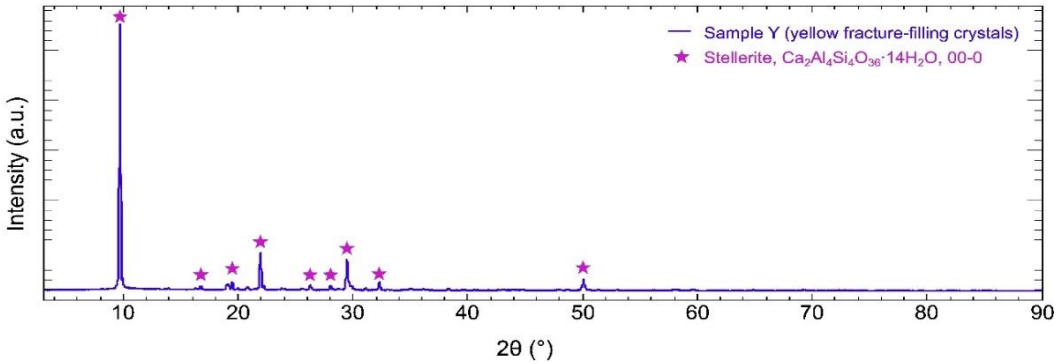

Figure 4 Diffractogram of yellow crystals from the fracture cavity (sample Y)

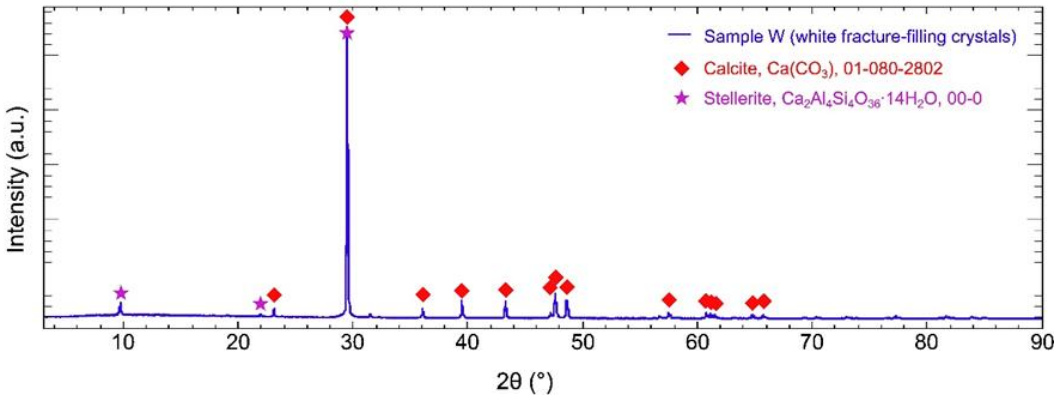

Figure 5 Diffractogram of white crystals from the fracture cavity (sample W)

3.2. Mineralogical assemblage in the green wall rock sample

The diffractogram of the green wall-rock sample (G) is presented in Figure 6. The XRPD analysis of the green wall-rock sample identified the following minerals:

1. quartz (SiO_2),
2. glauconite [$K(Fe,Al)_2(Si,Al)_4O_{10}(OH)_2$],
3. epistilbite [$Ca_2(Si_9Al_3)O_{24}\cdot 8H_2O$], and
4. clinochlore [$Mg_5Al(Si_3Al)O_{10}(OH)_8$].

Quartz is identified as α-quartz (ICDD 01-075-8321) [25]. The strongest diffraction maximum occurs at d = 3.3433 Å (011).

Glauconite is identified based on its basal reflection

at d = 9.948 Å (001), which closely matches the reference d = 10.018 Å (ICDD 00-063-0583) [26]. It is important to note that glauconite and celadonite have very similar layer structures and nearly identical basal spacings around 10 Å, as well as overlapping higher-order reflections. As a result, XRPD alone cannot unambiguously distinguish between these two minerals. Their identification typically requires chemical analysis, such as the Fe^{3+}/Fe^{2+} ratio and K content. The assignment to glauconite here is therefore based on peak positions and geological context, but should be considered tentative.

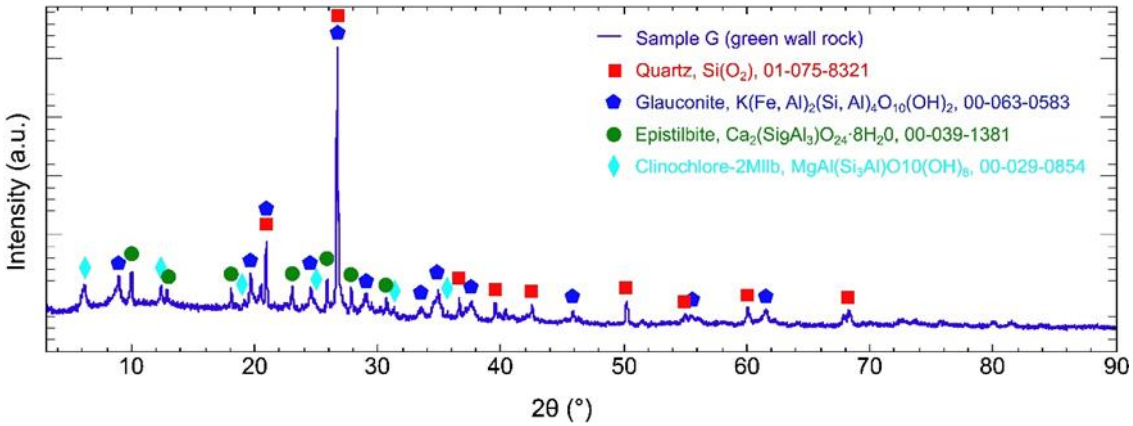

Figure 6 Diffractogram of green wall-rock sample (sample G)

Epistilbite is recognized by its characteristic low-angle reflection at d = 8.875 Å (020), which is in a good agreement with the reference d = 8.900 Å (ICDD 00-039-1381) [27].

Clinochlore (chlorite group, ICDD 00-029-0854) [28] is identified by its basal (001) hkl reflection at 6.10° 2θ (d = 14.48 Å) compared with the reference 6.22° (d = 14.20 Å).

3.3. Paragenetic sequence and formation history

The mineral assemblages observed in the wall rock and fracture infillings record a multistage post-depositional history reflecting the transition from early diagenetic to late low-temperature hydrothermal processes within the andesitic volcaniclastic deposits of the TMC. The host rock is an andesitic volcaniclastic unit rather than massive andesite, characterized by porous and initially unconsolidated volcaniclastic material [5], [22]. This lithology favored both early fluid–rock interactions within the porous medium and subsequent fracture-controlled mineralization.

The earliest stage is represented by authigenic glauconite, propylitic chlorite, and quartz in the wall-rock sample. Glauconite formed through low-temperature circulation of K- and Fe-bearing fluids in the porous volcaniclastic material during early diagenesis or low-grade hydrothermal alteration. Clinochlore is a typical propylitic alteration product of ferromagnesian phases. Quartz is largely inherited from the original volcaniclastic deposit as primary volcanic crystals incorporated during eruption, though minor secondary silicification may have occurred concurrently with chlorite formation. Together, these phases define the early alteration and diagenetic stage that preceded any significant fracturing.

A subsequent stage involved the development of a fracture within the already lithified volcaniclastic deposit, likely driven by tectonic stress or contraction during post-depositional cooling and compaction. At this point, the deposit had sufficient mechanical strength to sustain open fractures, creating new conduits for fluid flow distinct from the primary porosity.

Before mineralization of the main fracture occurred, local zeolitization of the wall rock took place, forming epistilbite within pores of the green volcaniclastic material. This phase represents a transitional stage between early diagenetic alteration and late fracture-controlled hydrothermal activity, reflecting continued low-temperature fluid flow through the porous host rock.

The final stage is characterized by low-temperature hydrothermal circulation through the main fracture, leading to mineral precipitation in a distinct zonal pattern: stellerite–stilbite zeolites were deposited first along the

fracture walls, followed by calcite filling the central part of the cavity. This sequence produced the characteristic sandwich-like texture observed in hand specimens and reflects the progressive evolution of hydrothermal fluids from zeolite to carbonate saturation under waning thermal conditions.

The complete paragenetic sequence can thus be summarized as follows:

- Early quartz (primary) + glauconite + chlorite alteration in porous volcaniclastics.
- Epistilbite formation in pores and microfractures during secondary zeolitization of wall rock.
- Fracture formation in lithified volcaniclastics.
- Zeolite (stellerite–stilbite) deposition on fracture walls.
- Calcite filling of the fracture core.

This multistage history highlights the interplay between depositional textures, early diagenetic processes, wall-rock zeolitization, structural fracturing, and late hydrothermal mineralization. It also clarifies the relative timing of quartz, glauconite, epistilbite, stellerite–stilbite, and calcite formation within the evolving hydrothermal system.

The mineral assemblages within the studied fracture and adjacent volcaniclastic rocks record hydrothermal processes fundamentally distinct from those responsible for porphyry Cu–(Au) mineralization. The Late Cretaceous ore-forming systems involved high-temperature, metal- and sulfur-rich fluids circulating at significant depths and pressures. These fluids, derived from magmatic sources, were capable of leaching and transporting Cu and Fe, precipitating pyrite, chalcopyrite, and associated alteration minerals within fracture and permeable zones [7], [14]. By contrast, the zeolites (stellerite–stilbite, epistilbite), glauconite, chlorite, and calcite in and around the fracture reflect later circulation of low-temperature, Ca–Na–HCO_3-dominated fluids under shallow crustal conditions. These fluids were essentially metal-poor and chemically buffered by the surrounding rocks, favoring zeolitization and carbonate precipitation. Their activity likely corresponds to Neogene or younger phases of regional geothermal circulation. Present-day hydrothermal activity is evidenced in Šarbanovac Spa (∼1 km from the study site), Sumrakovac Spa (3.7 km away), and Brestovac Spa (10 km away). This clear distinction in temperature, chemistry, and timing emphasizes the multiphase hydrothermal evolution of the TMC, in which late-stage, non-ore-forming fluid systems overprinted the earlier magmatic–hydrothermal environment that produced the region's world-class copper deposits.

4. Conclusions

The mineralogical and structural relationships observed in the Šarbanovac River bedrock exposure provide new insights into the late-stage hydrothermal evolution of the TMC. The host rock is an andesitic volcaniclastic unit that initially underwent early diagenetic alteration characterized by glauconitization and chloritization, with quartz largely preserved as primary volcanic detritus. Subsequent wall-rock zeolitization produced epistilbite in pores and microfractures, marking a transitional stage between early alteration and later hydrothermal activity. Fracturing of the lithified volcaniclastic deposit created pathways for low-temperature hydrothermal fluids, leading to sequential deposition of stellerite–stilbite along fracture walls, followed by calcite in the center.

The resulting zonal mineral assemblage and sandwich-like texture record a well-defined paragenetic sequence that integrates depositional, diagenetic, and structural processes. This sequence highlights the capacity of porous volcaniclastic lithologies to undergo multiple alteration stages before and during fracture-related mineralization. Furthermore, the study underscores the value of geomorphic windows, such as seasonally desiccated bedrock channels, for directly observing fracture-controlled mineral parageneses in their original geological context. Such observations are rare in the Timok region and provide complementary evidence to subsurface data, contributing to a more comprehensive understanding of the post-volcanic hydrothermal history of the TMC.

Acknowledgements

This work was supported by the Ministry of Science, Technological Development, and Innovation of the Republic of Serbia (Contract No. 451-03-137/2025-03/200131, and Contract No. 451-03-136/2025-03/200052).

5. References

[1] Melcher, F., Reichl, C. (2017) Economic geology of the Eastern and South-eastern European (ESEE) region. Berg- und Hüttenmännische Monatshefte, 162 (7), 238–244.

[2] Jelenković, R., Milovanović, D., Koželj, D., Banješević, M. (2016) The mineral resources of the Bor metallogenic zone: A review. Geologica

Carpathica, 67 (2), 143–155.
[3] Mladenović, A., Stojadinović, U., Cvetković, V., Prelević, D. (2023) Understanding geodynamics of the long-lasting Adria–Europe convergence: New constraints from the central Balkans. Geološki anali Balkanskoga poluostrva, 84 (1), 1–4.
[4] Velojić, M., Klimentyeva, D., von Quadt, A., Guillong, M., Melcher, F., Meisel, T., Prelević, D. (2023) New insights on the geochemical affinity and age of mineralized rocks in Timok magmatic complex, East Serbia. Geološki anali Balkanskoga poluostrva, 84 (1), 47–63.
[5] Banješević, M. (2010) Upper Cretaceous magmatic suites of the Timok Magmatic Complex. Geološki anali Balkanskoga poluostrva, 71, 13–22.
[6] Banješević, M., Cvetković, V., von Quadt, A., Obradović, D. Lj., Vasić, N., Pačevski, A., Peytcheva, I. (2019) New constraints on the main mineralization event inferred from the latest discoveries in the Bor Metallogenetic Zone (BMZ, East Serbia). Minerals, 9 (11), 672.
[7] Velojić, M., Jelenković, R., Cvetković, V. (2020) Fluid evolution of the Čukaru Peki Cu–Au porphyry system (East Serbia) inferred from a fluid inclusion study. Geologia Croatica, 73 (3), 197–209.
[8] Klimentyeva, D., Velojić, M., von Quadt, A., Hood, S. (2022) Interpretation of trace element chemistry of zircons from Bor and Čukaru Peki: Conventional approach and random forest classification. Geosciences, 12 (10), 396.
[9] Stojadinović, U., Toljić, M., Trivić, B., Pantović, R., Srećković-Batočanin, D., Krstekanić, N., Kostić, B., Velojić, M., Stefanović, J., Randjelović, N., Maleš, M. (2024) Geodynamics of basins above subducted slabs: An integrated modelling study of tectonics, sedimentation, and magmatism in the Timok Magmatic Complex. Geološki anali Balkanskoga poluostrva, 85 (2), 107–114.
[10] Gallhofer, D., von Quadt, A., Peytcheva, I., Schmid, S. M., Heinrich, C. A. (2015) Tectonic, magmatic, and metallogenic evolution of the Late Cretaceous arc in the Carpathian–Balkan orogen. Tectonics, 34 (8), 1813–1836.
[11] Milovanović, D., Karamata, S., Banješević, M. (2005) Petrology of alkali basalts of Zlot, Timok Magmatic Complex (Eastern Serbia). Tectonophysics, 410 (1–4), 501–509.
[12] Márton, E., Cvetkov, V., Banješević, M., Imre, G., Pačevski, A. (2024) Tectonic evolution of the Circum-Moesian orocline of the Carpatho-Balkanides: Paleomagnetic constraints. Journal of Geodynamics, 162, 102058
[13] Clark, A.H., Ullrich, T.D. (2004) ^{40}Ar–^{39}Ar age data for andesitic magmatism and hydrothermal activity in the Timok Massif, eastern Serbia: implications for metallogenetic relationships in the Bor copper–gold subprovince. Mineralium Deposita, 39 (3), 256–262.
[14] Xing, B., Liu, W., Xie, G., Xu, J., Zheng, W., Chen, L., Rao, D., Wang, H. (2025) Garnet geochronology and mineral geochemistry of the Veliki Krivelj porphyry-skarn Cu deposit, eastern Serbia: Implications for skarn formation and hydrothermal fluid evolution. Ore Geology Reviews, 186, 106841.
[15] Banješević, M. (2024) A review of the stratigraphic characteristics and age data of the main rock units in the Bor metallogenic zone (Timok Magmatic Complex). Journal of Mining and Metallurgy, Section A: Mining, 60 A, 1-10.
[16] Phillips, C. B., Masteller, C. C., Slater, L. J., Dunne, K. B. J., Francalanci, S., Lanzoni, S., Merritts, D. J., Lajeunesse, E., Jerolmack, D. J. (2021) The importance of threshold in alluvial river channel geometry and dynamics. EarthArXiv preprint, May 2021.
[17] Mueller, E. R., Smith, M. E., Pitlick, J. (2016) Lithology-controlled evolution of stream bed sediment and basin-scale sediment yields in adjacent mountain watersheds, Idaho, USA. Earth Surface Processes and Landforms, 41 (11), 1523–1537.
[18] Church, M. (2006) Bed material transport and the morphology of alluvial river channels. Annual Review of Earth and Planetary Sciences, 34, 325–354.
[19] O'Connor, J. E., Mangano, J. F., Anderson, S. W., Wallick, J. R., Jones, K. L., Keith, M. K. (2014) Geologic and physiographic controls on bed-material yield, transport, and channel morphology for alluvial and bedrock rivers, western Oregon. GSA Bulletin, 126 (3–4), 377–397.
[20] Bartels, G. K., dos Reis Castro, N. M., Loguercio Collares, G., Fan, F. M. (2021) Performance of bedload transport equations in a mixed bedrock–alluvial channel environment. Catena, 199, 105108.
[21] Fernández, R., Parker, G., Stark, C. P. (2019) Experiments on patterns of alluvial cover and bedrock erosion in a meandering channel. Earth Surface Dynamics, 7, 949–968.
[22] Veselinović et al. (1967) Tumač I geološka karta,

list Zaječar, OGK SFRJ 1:100000 Savezni geol. Zavod, Beograd, pp 65.
[23] Galli, E., Passaglia, E. (1973) Stellerite from Villanova Monteleone, Sardinia. Lithos, 6 (1), 83–89.
[24] Antao, S. M., Hassan, I. (2010) Temperature dependence of the structural parameters in the transformation of aragonite to calcite, as determined from in situ synchrotron powder X-ray-diffraction data. The Canadian Mineralogist, 48, 1225–1236.
[25] Ikuta, D., Kawame, N., Banno, S., Hirajima, T., Ito, K., Rakovan, J. F., Downs, R. T., Tamada, O. (2007) First in situ X-ray identification of coesite and retrograde quartz on a glass thin section of an ultrahigh-pressure metamorphic rock and their crystal structure details. American Mineralogist, 92 (1), 57–63.
[26] Li, X., Cai, Y., Hu, X., Huang, Z., Wang, J. (2012) Mineralogical characteristics and geological significance of Albian (Early Cretaceous) glauconite in Zanda, southwestern Tibet, China. Clay Minerals, 47, 45–58.
[27] Gottardi, G., Galli, E. (1985) Natural Zeolites. Springer-Verlag, Berlin, 338 pp.
[28] Post, J. L., Plummer, C. C. (1972) The chlorite series of Flagstaff Hill area, California: A preliminary investigation. Clays and Clay Minerals, 20 (5), 271–283.

PARAGENEZA STELERITA-STILBITA I KALCITA U PUKOTINSKOJ ŠUPLJINI U ANDEZITSKIM VULKANOKLASTIČNIM STENAMA TIMOČKOG MAGMATSKOG KOMPLEKSA

D. Medić[1#], Z. Štirbanović[1], M. Banješević[1], V. Nedelkovski[1], S. Stanković[1], A. Cvetković[1], S. Đorđievski[2],

[1]Univerzitet u Beogradu, Tehnički fakultet u Boru, Bor, Srbija
[2]Institut za rudarstvo i metalurgiju, Bor, Srbija

Primljen: 3. oktobra 2025.; Prihvaćen: 2. decembra 2025.

Izvod

Timočki magmatski kompleks (TMK) predstavlja deo Apusensko–Banatsko–Timočko–Srednjogorskog magmatskog luka u okviru Tetiskog metalogenetskog pojasa, koji sadrži svetski poznata porfirska i epitermalna ležišta bakra i zlata. U stenovitom koritu Šarbanovačke reke (centralni deo TMK), sezonsko isušivanje je otkrilo pukotinu unutar gornjokrednih andezitskih vulkanoklastičnih stena, gde su zapaženi beli i žuti mineralni agregati unutar same pukotine, i zeleni mineralni agregati u okolnoj steni. Rezultati ispitivanja metodom rendgenske difrakcije na polikristalnom uzorku (prahu) (XRPD) pokazali su da se žuti kristali sastoje od zeolita stelerita-stilbita, dok su beli kristali sačinjeni od kalcita. Okolna zelena stena sadrži kvarc, glaukonit, klinohlor i epistilbit. Kvarc predstavlja reliktna magmatska zrna uklopljena u vulkanoklastični materijal, dok glaukonit i klinohlor odražavaju ranu dijagenetsku do propilitsku alteraciju. Epistilbit se javlja u porama i mikropukotinama, ukazujući na lokalnu zeolitizaciju stene koja je prethodila glavnoj mineralizaciji pukotine. Stelerit-stilbit se najpre nataložio na zidovima pukotine, nakon čega je kalcit ispunio središnji deo pukotine, formirajući karakterističnu slojevitu („sendvič") teksturu. Ovi nalazi dokumentuju višestepenu paragenetsku evoluciju koja obuhvata ranu dijagenetsku alteraciju poroznog vulkanoklastičnog materijala, sekundarnu zeolitizaciju, tektonski formirane pukotine i kasniju niskotemperaturnu hidrotermalnu mineralizaciju. Ovo istraživanje predstavlja redak primer pukotinski kontrolisane parageneze zeolita i karbonata očuvane „in situ" u vulkanoklastičnim stenama TMK.

Ključne reči: *vulkanoklastiti, andezit, pukotina, stilbit, stelerit, kalcit.*